



Inter-specific variability in demographic processes affects abundance–occupancy relationships

Bilgecan Şen¹ · H. Reşit Akçakaya¹

Received: 4 May 2021 / Accepted: 20 November 2021

© The Author(s), under exclusive licence to Springer-Verlag GmbH Germany, part of Springer Nature 2021

Abstract

Species with large local abundances tend to occupy more sites. One of the mechanisms proposed to explain this widely reported inter-specific relationship is a cross-scale hypothesis based on dynamics at the population level. Called the vital rates mechanism; it uses within-population demographic processes of population growth and density dependence to predict when inter-specific abundance–occupancy relationships can arise and when these relationships can weaken and even turn negative. Even though the vital rates mechanism is mathematically simple, its predictions has never been tested directly because of the difficulty estimating the demographic parameters involved. Here, using a recently introduced mark-recapture analysis method, we show that there is no relationship between abundance and occupancy among 17 bird species. Our results are consistent with the predictions of the vital rate mechanism regarding the demographic processes that are expected to weaken this relationship. Specifically, we find that intrinsic growth rate and local abundance are not correlated, and density dependence strength shows considerable variation across species. Variability in density dependence strength is related to variability in species-level local average abundance and intrinsic growth rate; species with lower growth rate have higher abundance and are strongly regulated by density dependent processes, especially acting on survival rates. More generally, our findings support a cross-scale mechanism of macroecological abundance–occupancy relationship emerging from density-dependent dynamics at the population level.

Keywords Density-dependence · Population demography · Intrinsic growth · Mark-recapture · Macroecology

Introduction

Exploring ecological processes and interactions across scales of biological organization allows a deeper understanding of patterns of biodiversity. One well-documented macroecological pattern is the abundance–occupancy relationship: across phylogenetically similar species, local average abundance and proportion of sites occupied are positively correlated (Hanski 1982; Bock and Ricklefs 1983; Brown 1984, 1995; Gaston and Blackburn 2000). This pattern has been observed in a variety of taxa, such as mammals (Blackburn et al. 1997), birds (Lacy and Bock 1986; Blackburn et al.

1997), butterflies (Conrad et al. 2001), mollusks (Russell and Lindberg 1988), and plants (Guo et al. 2000). A meta-analysis on abundance–occupancy relationships found an overall positive correlation but also reported high variability in the strength of this relationship across species realms (Blackburn et al. 2006). Some species groups even show zero or negative correlation between abundance and occupancy (Novosolov et al. 2017), which may be the result of an ecological process (Symonds and Johnson 2006; Reif et al. 2006; Ferenc et al. 2016; Freeman 2019), or an artifact of the particular metrics used to represent abundance and occupancy (Wilson 2008).

Several mechanisms have been proposed to explain the positive relationship between abundance and occupancy (reviewed by Gaston et al. 1997 and Borregaard and Rahbek 2010). Among these, one mechanism, known as "vital rates", is notable for being the only one that explains this macroecological relationship with population demography. Proposing the vital rates mechanism, Holt et al. (1997) argued

Communicated by Janne Sundell.

✉ Bilgecan Şen
bilgecan.sen@gmail.com

¹ Department of Ecology and Evolution, Stony Brook University, Stony Brook, NY 11794, USA

that the positive correlation between number of occupied sites and local average abundance across species is a consequence of the relationship among population abundance, intrinsic population growth rate (r), and occupancy. Vital rates mechanism can be summarized in two parts. First, it can be shown that equilibrium abundance is related to intrinsic growth and density dependence using an alternative parameterization of logistic growth equation (Kuno 1991; Holt et al. 1997):

$$\bar{N} = \bar{r} / \mu, \quad (1)$$

where \bar{N} is the equilibrium abundance, \bar{r} is the average intrinsic growth rate in a temporally variable environment, and μ is the per capita decrease in \bar{r} . Here, we use an age structure with two age classes so intrinsic growth can be written as follows:

$$r = \log (S_{ad} + S_{juv} \cdot F), \quad (2)$$

where S_{ad} and S_{juv} are adult and juvenile survival, respectively, and F is fecundity (number juveniles per adults) when population density is close to 0.

Second, if source-sink dynamics are not the primary mode of occurrence, a species exist only in sites with $r > 0$. When r is determined by a uniform environmental gradient, any environmental factor that increases r will also increase the number of occupied sites (Fig. 1). Higher r will also lead to higher equilibrium abundances (Eq. 1), establishing the connection between occupancy and abundance.

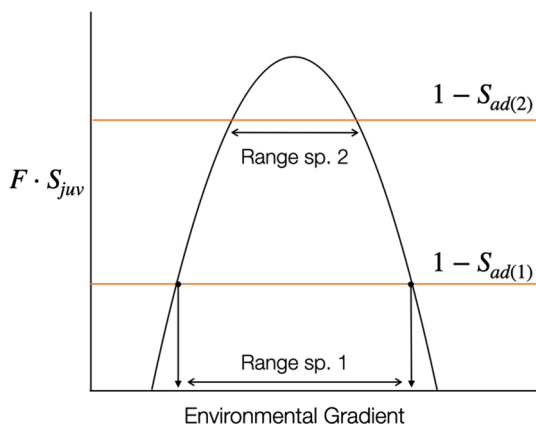


Fig. 1 A generalization of Holt et al. (1997)'s Fig. 1a to species with two age classes. Equation 2 dictates that species can only exist in a site if $S_{juv} \cdot F$ is larger than $1 - S_{ad}$ (death rate). This is a simplified case where two species have different adult survival rates and but equal $S_{juv} \cdot F$ that varies across an environmental gradient. Species with higher death rate, and therefore lower growth rate will be confined to a narrower range

Differences in intrinsic growth rates among species will lead to the observed positive inter-specific relationship between abundance and occupancy. This general system of population dynamics, in other words the vital rates mechanism, has specific predictions for when positive abundance-occupancy relationships should arise and when they should weaken or disappear. We summarize these predictions of vital rates mechanism under the following three headings:

1. *Relationship between intrinsic growth rate and occupancy among species*

Intrinsic growth rate plays a central role in vital rates mechanism because it is the link between abundance and occupancy. So, if there is a positive abundance-occupancy relationship among a group of species and if the vital rates mechanism is the major process that determines this relationship, there should also be a positive association between intrinsic growth rate and occupancy. Alternatively, if intrinsic growth rate and occupancy are not closely related then we would expect a weak abundance-occupancy relationship.

2. *Relationship between intrinsic growth rate and abundance among and within species*

As stated above, in vital rates mechanism, intrinsic growth rate relates occupancy to abundance. So, if there is positive abundance-occupancy relationship in a group of species, and if the vital rates mechanism is the major process that determines this relationship, populations with higher growth rates should also have higher abundances, and species with higher average growth rates should have higher average abundances. If abundance and intrinsic growth rate do not show positive correlation, we would expect a weak abundance-occupancy relationship according to vital rates mechanism

3. *Variability of density dependence strength among species.*

If density dependence, parameterized as per capita decrease in intrinsic growth (μ in Eq. 1), is variable across species, the positive relationship between abundance and intrinsic growth rate will be lost, which can weaken or completely disassociate abundance and occupancy. Additionally, Holt et al. (1997) hypothesized that “[a] species with small r but weak density dependence can obtain enormous local abundances compared to another species with large r but intense density dependence”. In this scenario, differences in density dependence strength breaks the expected positive correlation between abundance and intrinsic growth and weakens the abundance occupancy relationship. Accordingly, if there is a positive abundance-occupancy relationship in a group of species, and if the vital rates mechanism is the major process that determines this relationship, density dependence strength across these species should

be similar and should not be correlated with intrinsic growth rate and abundance. However, if density dependence strength is positively correlated with intrinsic growth rate and negatively correlated with abundance (as in the scenario above), we should expect a weaker abundance–occupancy relationship.

Here, we use mark-recapture data to estimate the vital rates and population abundances of 17 bird species, and explicitly test the aforementioned predictions of Holt et al. (1997)'s vital rates mechanism. While these predictions have been tested using proxy parameters, for example, the skewness in population size distributions (Freckleton et al. 2006), to our knowledge, they have never been explicitly tested with the estimation of the demographic parameters involved in the mechanism itself.

Materials and methods

Data: mapping avian productivity and survivorship (MAPS)

MAPS is a collaborative mark-recapture program initiated and organized by the Institute for Bird Populations (IBP) since 1989 across 1200 bird banding stations with mist nets in US and Canada. We had only access to environmental data (explained below) from conterminous United States and to MAPS data from 1992 to 2008, so we limited captures to this region and time period. Additionally, we only used captures between May and August that corresponds to the breeding season of the species we used. We considered first year individuals (MAPS age code 2 and 4) as juveniles, and all older individuals (MAPS age code 1, 5, 6, 7, and 8) as adults. We applied Albert et al. (2016)'s suggested filters for MAPS dataset to both adults and juveniles. There were 62 species in total that passed this filtering process. However, we applied CJS-pop to only 42 species due to computational limitations, in which maximum model convergence time was 1 week; we did not analyze species with sample sizes that required longer run time. For each species, we treated separate MAPS locations (a cluster of mist-netting and banding stations) to be independent breeding populations. We only included data from populations which have been monitored for at least 5 years (not necessarily consecutively)

Data: environmental covariates

We used the downscaled Maurer gridded data (Maurer et al. 2002) which were shown to be superior to several other alternatives in terms of its closeness to observed measurements (Behnke et al. 2016), to calculate the ten metrics used as environmental covariates in the modeling framework explained

below: annual mean temperature, mean diurnal range, mean temperature of wettest quarter, annual precipitation, precipitation of warmest quarter, maximum consecutive dry days, maximum consecutive 5-day precipitation total for March, standard deviation in daily temperatures for March, total precipitation in May, and number of dry days in April. We used annual aggregates of these metrics when building mark-recapture models. Each MAPS location was assigned the covariate values of the grid cell it was located in. If the mist-netting stations of a location was distributed across multiple grid cells we assigned the average value of the covariates across those grid cells to that location. We repeated this process for every year between 1992 and 2008 for every MAPS location, creating a time series of weather variables at each location.

Mark-recapture analysis framework

We used the framework developed by Ryu et al. (2016), which employs robust design mark-recapture data, to estimate population vital rates (survival and fecundity) as well as density-dependence and process variance in these vital rates (temporal or spatial variability). Models were fit using Bayesian statistics and JAGS as the MCMC sampler. Below, we focus on how these vital rates and capture probabilities are used to estimate intrinsic growth rate and abundance. A more detailed explanation of the framework can be found in Appendix S2.

We model survival and fecundity as functions of environmental covariates in addition to density dependence. An example model structure, here illustrated for $\phi_{x,k,t}$, the survival probability of a stage x individual, at population k , and at year t , with two environmental covariates is given as follows:

$$\text{logit}(\phi_{x,k,t}) = \alpha_x - \beta_1 \cdot D_{k,t} + \beta_2 \cdot W_{1,k,t} + \beta_3 \cdot W_{2,k,t} + \epsilon_t \quad (3a)$$

$$\epsilon_t \sim \text{Normal}(0, \sigma_s^2), \quad (3b)$$

where α_x is the survival probability of a stage x individual in logit scale at mean population size and at mean of environmental covariates W_1 and W_2 ; β_1 is the change in survival in logit scale with one unit change in population density index; D is the population density index at population k , and at year t (See Appendix S2 for density index calculation); β_2 and β_3 are the change in survival in logit scale with one unit change in W_1 and W_2 , respectively; ϵ_t is the temporal random effect at year t , and σ_s^2 is the temporal process variance of survival at logit scale; $x = 1, 2, \dots, X$; $k = 1, 2, 3, \dots, K$; $t = 1, 2, 3, \dots, T$. We denote $x = 1$ as juveniles and, $x = 2$ as adults.

Similarly, fecundity $F_{k,t}$ at population k and year t can be modelled as follows:

$$\log(F_{k,t}) = \theta - \zeta_1 \cdot D_{k,(t-1)} + \zeta_2 \cdot W_{1,k,t} + \zeta_3 \cdot W_{2,k,t} + \omega_t \quad (4a)$$

$$\omega_t \sim \text{Normal}\left(0, \sigma_f^2\right), \tag{4b}$$

where θ is the average fecundity in log scale at mean population size and at mean of environmental covariates W_1 and W_2 ; ζ_1 is the change in fecundity in log scale with one unit change in population density index; ζ_2 and ζ_3 are the changes in fecundity in log scale with one unit change in W_1 and W_2 , respectively; ω_t is the temporal random effect at year t , and σ_f^2 is the temporal process variance of fecundity in log scale. This framework is set so that when a population is at its average density index value (e.g. at carrying capacity), the growth rate calculated by fecundity, adult survival, and juvenile survival is 0 (See [Appendix S2](#) for details on estimation of fecundity).

Because this framework is an extended version of a typical Cormack–Jolly–Seber (CJS) method (Ryu et al. 2016), capture probability $p_{x,k,t,h}$ of a stage x individual at population k , year t , and month h is explicitly modelled alongside vital rates as a function of capture effort as follows:

$$\text{logit}(p_{x,k,t,h}) = \gamma_x + \delta \cdot E_{k,t,h}, \tag{5}$$

where γ_x is the monthly capture probability on logit scale of a stage x individual at mean capture effort; δ is the change in monthly capture probability on logit scale with one unit change in capture effort; E is the capture effort, which is calculated as total mist netting hours per month in a population; $h = 1, 2, 3, \dots, H$.

To prevent overfitting and fasten the convergence of mark-recapture models, we reduced the number of covariates with principal component analysis (PCA) and used the number of principle components that cumulatively explains 80% of the variation. We applied PCA separately to each species using the time series of weather covariates from the MAPS locations a given species was captured in.

Estimating demographic parameters

Intrinsic growth rate

Intrinsic population growth rate is the density independent population growth rate. While the exact meaning depends on the estimation method (Lynch and Fagan 2009), it represents the theoretical maximum of a population’s ability to grow in size when population density is close to 0. To estimate intrinsic growth rate at a given population and year, we set density to 0 and estimate survival and fecundity only as functions of environmental covariates. We use posterior means of parameters and omit process variance

when estimating survival and fecundity. Then, we use Eq. 2 to estimate intrinsic growth rate at population k and year t and calculate the average growth across T years as follows:

$$\bar{r}_k = \frac{\sum_{t=1}^T r_{k,t}}{T}. \tag{6}$$

Finally, to estimate species level intrinsic growth rate we take the average of population level growth rates as follows:

$$\bar{r} = \frac{\sum_{k=1}^K \bar{r}_k}{K}, \tag{7}$$

where \bar{r} is a vector with population level intrinsic growth rates.

We only used species with a negative density-dependence effect on growth rate (growth rate at density index 2 was lower than growth rate at density index 0). Intrinsic growth rate is not defined for circumstances in which increasing density also increases the population growth; in such a case intrinsic growth rate loses its meaning as a theoretical maximum. Additionally, positive density dependence effects are biologically meaningful only when Allee effects are considered. Because we are not modelling Allee effects with this framework, we removed species that showed a positive density dependence effect on growth rate from further analysis.

Population size

The monthly capture probabilities obtained from CJS-pop are used to calculate the yearly capture probabilities, and these in turn are used to estimate the expected size of each population in each year. Yearly capture probabilities for each adult and juvenile in a given year and population is calculated as follows:

$$p_{x,k,t}^* = 1 - \prod_{h=1}^4 (1 - p_{x,k,t,h}), \tag{8}$$

where $p_{x,k,t}^*$ is the probability that a stage x individual will be captured at least once in 4 months of the breeding period at year t and population k .

Using the heuristic estimator for population size with a correction for years with 0 captures (Dail and Madsen 2011), the numbers of adults and juveniles can be derived as follows:

$$N_{x,k,t} = \frac{n_{x,k,t}}{p_{x,k,t}^*} + \frac{(1 - p_{x,k,t}^*)}{p_{x,k,t}^*}, \tag{9}$$

where $n_{x,k,t}$ is the number of captured stage x individuals at population k and year t , and $N_{x,k,t}$ is the expected number of stage x individuals of the same population and year combination. Average total population size for each population is estimated as follows:

$$\bar{N}_k = \frac{\sum_{t=1}^T N_{1,k,t} + N_{2,k,t}}{T \cdot m_k}, \quad (10)$$

where T is the number of sampling years of a population. MAPS locations can have different number of stations, we standardize total population size by dividing by the number of stations of population k , m_k . We estimate the species level population abundance as the median population size across all populations as follows:

$$\bar{\bar{N}} = \text{median}(\bar{N}), \quad (11)$$

where \bar{N} is a vector with average population sizes.

Occupancy

There are 495 MAPS locations across US in the dataset we used for this analysis. The number of MAPS locations a species was captured in provides information about the distribution and occupancy of a species. Different measures of occupancy affect the strength of estimated abundance–occupancy relationship (Borregaard and Rahbek 2010). Here, we define occupancy using two different measures: (1) geographic extent calculated as 100% minimum convex polygon of all the stations in which a species was captured; (2) number of different populations (MAPS locations) in which a species was captured.

Per-capita decrease in growth

We calculated a species level per-capita decrease in intrinsic growth (μ) using \bar{N} and \bar{r} in Eq. 1. μ , in this case, represents the overall effect of density dependence on survival and fecundity. We calculate coefficient of variation of μ to represent its variability and for a quantitative investigation of whether density dependence is variable across species.

Testing the predictions of vital rates mechanism

For each test below we estimate the Pearson's correlation coefficient (ρ) and report the posterior probability of the prediction being tested, $P(\rho > 0)$, and the Bayes factor against

the null hypothesis that $\rho = 0$ (Jeffreys 1983). Bayes factors indicate how probable a hypothesis is in comparison to a null hypothesis. We weight evidence against the null hypothesis using the following thresholds suggested by Kass and Raftery (1995): No evidence against null when Bayes factor is below 1, anecdotal evidence when between 1 and 3, positive evidence when between 3 and 20, and strong evidence when larger than 20.

Abundance–occupancy relationship: Between species-level median abundance (\bar{N}) and each of the two metrics of occupancy, across species.

Relationship between intrinsic growth rate and occupancy: Between species-level median intrinsic growth rate (\bar{r}) and each of the two metrics of occupancy, across species.

Relationship between intrinsic growth rate and abundance within species: Between population-level abundance (\bar{N}) and population level intrinsic growth rate (\bar{r}), across populations, separately for each species.

Relationship between intrinsic growth rate and abundance among species: Between species-level median intrinsic growth rate (\bar{r}) and species-level median abundance (\bar{N}), across species.

Variability of density dependence strength among species: Among density dependence strength in both survival and fecundity (β and ζ , respectively), species-level average intrinsic growth rate (\bar{r}), and species-level average abundance \bar{N} .

Because we use uniform priors on ρ (Uniform $(-1, 1)$), posterior probability estimates above or below 0.5 can also be considered as a measure of evidence obtained from data regarding the prediction being tested. Detailed information on priors and model specifications of all Bayesian models used in this analysis can be found in Appendix S2. We use the R package BayesFactor for calculating Bayes factors (Morey and Rauder, 2018). R code for data manipulation and JAGS code for the mark-recapture framework are available at <https://github.com/bilgecansen/VitalRatesTest>.

Results

Of the 42 species analyzed, 34 yielded posterior distributions that converged ($\hat{R} < 1.1$ for all parameters). Of these 34 species, only 17 had an overall negative density dependence effect on growth rate (Table 1). Among these 17 species, population size showed a right skewed distribution with many small and few large populations (Appendix S1: Fig. S1a). The majority of these populations have $\bar{r} > 0$ with unimodal distribution that is centered on 0.14 (Appendix S1: Fig. S1b).

Table 1 List of the 17 selected species to be used in testing the vital rates mechanism

4-letter code	English name	Scientific name	Migration	Time series length	Number of populations	Generation length	Per capita decrease in growth
ACFL	Acadian flycatcher	<i>Empidonax virescens</i>	Migrant	11	54	3.7	0.0006
BRCR	Brown creeper	<i>Certhia americana</i>	Resident	13.8	43	3.3	0.0134
CACH	Carolina chickadee	<i>Poecile carolinensis</i>	Resident	11	62	4.3	0.0047
CALT	California towhee	<i>Melospiza crissalis</i>	Resident	9.6	20	4.3	0.0007
DOWO	Downy Woodpecker	<i>Dryobates pubescens</i>	Resident	11.4	167	4.7	0.0062
HAWO	Hairy woodpecker	<i>Dryobates villosus</i>	Resident	13.1	84	3.1	0.0023
HUVI	Hutton's vireo	<i>Vireo huttoni</i>	Resident	14.1	18	4.2	0.0341
INBU	Indigo bunting	<i>Passerina cyanea</i>	Migrant	10.5	94	4.1	0.0007
LISP	Lincoln's sparrow	<i>Melospiza lincolnii</i>	Migrant	13	28	3.6	0.0078
MOCH	Mountain chickadee	<i>Poecile gambeli</i>	Resident	13.7	23	4.2	0.0011
RCSP	Rufous-crowned Sparrow	<i>Aimophila ruficeps</i>	Resident	9.4	12	3.7	0.002
REVI	Red-eyed vireo	<i>Vireo olivaceus</i>	Migrant	10.7	110	4.2	0.0003
SPTO	Spotted towhee	<i>Pipilo maculatus</i>	Resident*	10.8	69	4.1	0.002
TUTI	Tufted titmouse	<i>Baeolophus bicolor</i>	Resident	10.9	94	3.8	0.0068
WEWP	Western wood-pewee	<i>Contopus sordidulus</i>	Migrant	12	63	3.4	0.0056
WREN	Wrentit	<i>Chamaea fasciata</i>	Resident	11.4	29	5.2	0.0063
YBCH	Yellow-breasted chat	<i>Icteria virens</i>	Migrant	11	76	3.9	0.0086

Migration: status indicate whether migratory or resident populations of a species were used in the analysis (*shows a species with a mix of resident and migratory populations in which case majority of the populations were resident). Time series length: Average time series length in years across populations of a species. Number of populations: Number of MAPS locations as species was captured in. Per-capita decrease in growth: A species level metric calculated using \bar{N} and \bar{r} in Eq. 2. Generation length is in years and was obtained from IUCN Red List (IUCN 2021)

We found no evidence that species level abundance (\bar{N}) is correlated with geographic extent ($\rho = 0.06$, $P(\rho > 0) = 0.52$, $B_0 = 0.4$; Fig. 2a) and with number of populations ($\rho = 0.26$, $P(\rho > 0) = 0.87$, $B_0 = 0.71$; Fig. 2b). Similarly, there was no evidence of a positive relationship between species level intrinsic growth rate (\bar{r}) and geographic extent ($\rho = 0.11$, $P(\rho > 0) = 0.68$, $B_0 = 0.44$; Fig. 3a), and number of populations ($\rho = 0.09$, $P(\rho > 0) = 0.65$, $B_0 = 0.43$; Fig. 3b).

There was a positive relationship between population-level intrinsic growth rate (\bar{r}) and population abundance (\bar{N}) for 13 out of 17 species (Fig. 4). Four of these species had anecdotal evidence that ρ was not 0 ($1 < B_0 < 3$), and one of them showed decisive evidence ($B_0 > 100$). The remaining 8 species showed no evidence of a relationship between \bar{r} and \bar{N} . Downy Woodpecker (DOWO) had the highest correlation coefficient with the lowest uncertainty ($\rho = 0.42$, $(0.31 - 0.53)$ $B_0 > 100$). Wrentit (WREN) was the only species with negative relationship between \bar{r} and \bar{N} that also suggested positive evidence ($B_0 = 4.68$; Fig. 4).

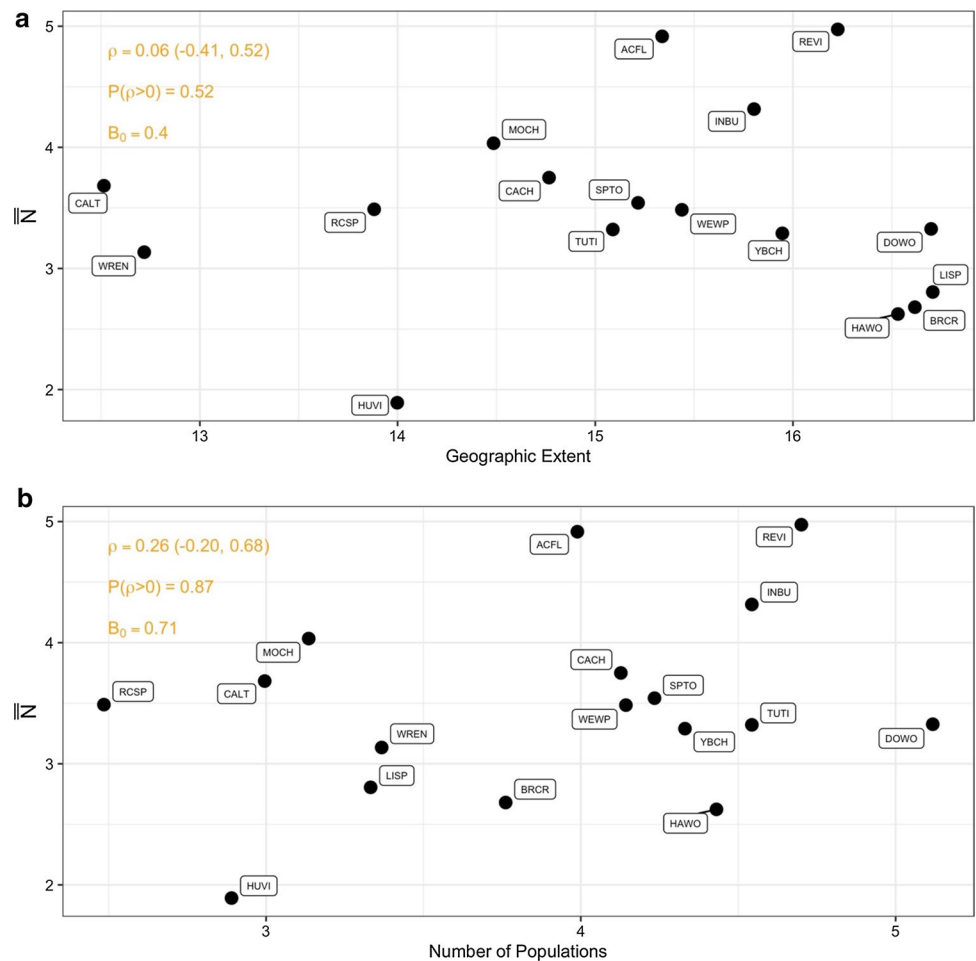
We found a moderately strong negative correlation between \bar{r} and \bar{N} ($\rho = -0.46$) indicating a very low probability of a positive relationship ($P(\rho > 0) = 0.01$), and anecdotal evidence against $\rho = 0$ ($B_0 = 2.76$; Fig. 5). There was

a moderately strong negative correlation between density dependence strength in survival (β) and \bar{N} , and between β and \bar{r} , which showed positive and strong evidence against $\rho = 0$ ($B_0 = 9.09$ and $B_0 = 27.6$, respectively; Fig. 6a and c) Relationship between density dependence in fecundity (ζ) and \bar{N} and \bar{r} showed no such evidence ($B_0 = 0.90$ and $B_0 = 0.39$; Fig. 6b and d) and the estimates of correlation coefficients were indistinguishable from 0.

Discussion

The vital rates mechanism explicitly links intrinsic population growth and density-dependent population regulation with the emerging relationship between abundance and occupancy on a macroecological scale. In doing so, however, it not only provides a mechanistic, population-level explanation for the emergence of the widely reported positive abundance-occupancy relationships, but also predicts conditions under which occupancy and abundance will be unrelated. Here, we show that a group of 17 bird species do not have a positive abundance-occupancy relationship (Fig. 2) and that this weak relationship might be caused by the fact that intrinsic growth rate is not acting as an intermediary between occupancy and abundance, as

Fig. 2 Correlations between species level median abundance (\bar{N}) and metrics of occupancy. Every point represents a single species. ρ is the Pearson's correlation coefficient and its 95% credible interval is in parenthesis. $P(\rho > 0)$ indicates the probability that there is a positive correlation between two parameters. B_0 is the bayes factor against the null hypothesis that $\rho = 0$



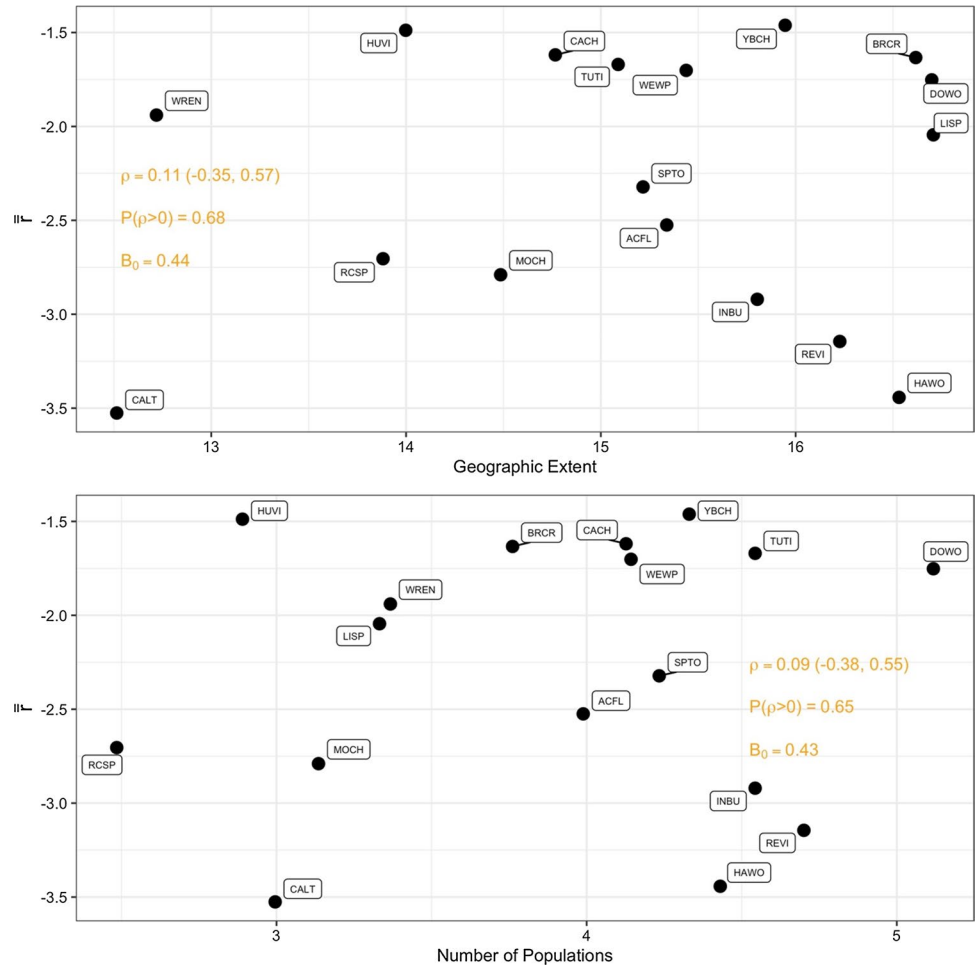
demonstrated by the following three lines of evidence: (1) population growth rates of these species appear unrelated to their range sizes and occupancy (Fig. 3), (2) intrinsic growth rates of these species are generally not related to their abundances at the population level (Fig. 4), and (3) there is a negative relationship between species-level growth rate and species-level abundance (Fig. 5) which is also associated with, and potentially emerge from, differences in density dependence strengths of vital rates (Table 1; Fig. 6). We discuss these relationships in detail below.

Variability in per-capita decrease in growth (μ) shows, on average, how much intrinsic growth rate on log scale would decrease per added individual per station, assuming that growth will be 0 when population reaches \bar{N} . Standardization of this metric per station is important because each population might consist of different number of stations, leading to different sampling area or sampling effort for each population. μ is highly variable with a coefficient of variation of 131% across 17 species with negative density dependence (Table 1). μ is especially high for Hutton's Vireo (0.034) compared to other species. If we

remove Hutton's Vireo the CV is reduced to 84%. Holt et al. (1997) never quantified the effect of variability in density dependence on abundance-occupancy relationship; however, these CV estimates can be put into context by comparing the variability of intrinsic growth rates among populations. For example, Brown Creeper's CV of growth rates among its populations is the highest across 17 species with 36%. So, the species level per-capita decrease of growth is at least 2.3 times more variable than population level intrinsic growth. The variability of density dependence that we report supports the vital rates mechanism's qualitative prediction that high variability should weaken the positive abundance-occupancy patterns.

This variability in density dependence can also emerge from different macroecological patterns. For example, a trade-off between intrinsic population growth and abundance is expected if fast growth is associated with stronger density dependence (Holt et al. 1997). Among the 17 bird species with negative density dependence in this study, there is anecdotal evidence for such a trade-off between intrinsic growth rate and abundance (Fig. 5). Hairy Woodpecker (HAWO) stands out as an outlier in this relationship and

Fig. 3 Correlations between species level median intrinsic growth rate (\bar{r}) and metrics of occupancy. Every point represents a single species with the corresponding 4-letter code. ρ is the Pearson's correlation coefficient and its 95% credible interval is in parenthesis. $P(\rho > 0)$ indicates the probability that there is positive correlation between two parameters. B_0 is the bayes factor against the null hypothesis that $\rho = 0$



when removed Bayes factor increases to 13.7 and suggests positive evidence for a non-zero relationship. This species-level trade-off is potentially driven by density-dependent population regulation because there is positive evidence that stronger density dependence is associated with higher growth and lower abundance (Fig. 6). The framework we used estimates density dependence strengths for survival and fecundity separately (Ryu et al. 2016). It revealed subtler patterns of density-dependent population regulation compared to Holt et al. (1997), which only used a single density dependence effect on population growth. The trade-off between high abundance and high growth is mostly driven by density dependence acting on survival, in which species with higher abundance and low growth are regulated by weaker density dependence, and species with higher growth but lower abundance are regulated by stronger density dependence. There is no evidence for such pattern in density dependence acting on fecundity. We are not aware of any other study exploring these patterns, so a better understanding of the relationship of density dependence with other demographic parameters, and the macroecological

patterns they might cause, requires further research in other taxonomic groups.

The detection of density dependence from time series data is affected by both data related issues (for example sample size or time series length) and the actual ecological process of intra-specific interactions. We found no evidence that favors one over the other across 34 species with a negative or positive density dependence. We compared average time series length, number of populations, generation length, strength of process variance on survival and fecundity, response to environmental change (slopes starting with β_2 and ζ_2), variability of abundance in a time series (in the form of CV), and capture probability of adults and juveniles between groups of species with an overall negative density dependence and positive density dependence using *t*-tests (Figs S2–S10). None of the comparisons showed any evidence for difference between the groups as all Bayes factors were below 1. We found anecdotal evidence with a contingency table analysis that it was more likely to detect negative density dependence for resident species ($B_0 = 1.65$). For some migratory species the density of their

Fig. 4 Correlation between population level abundance (\bar{N}) and intrinsic growth rate (\bar{r}) for each species (see Table 1 for species abbreviations). The orange dot indicates the mean of the posterior distribution of Pearson's correlation coefficient (ρ). Black lines are the 50% credible intervals and gray lines are 95% credible intervals of the posterior distributions. Numbers next to species codes is Bayes factors against the null hypothesis that $\rho = 0$

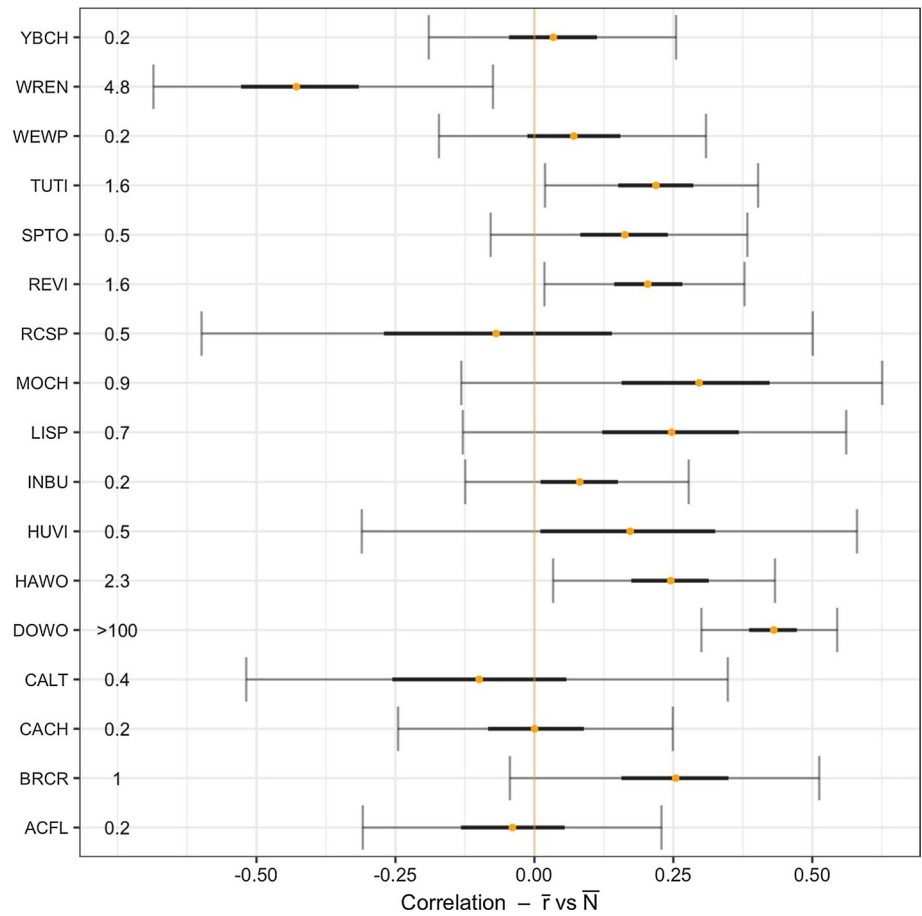
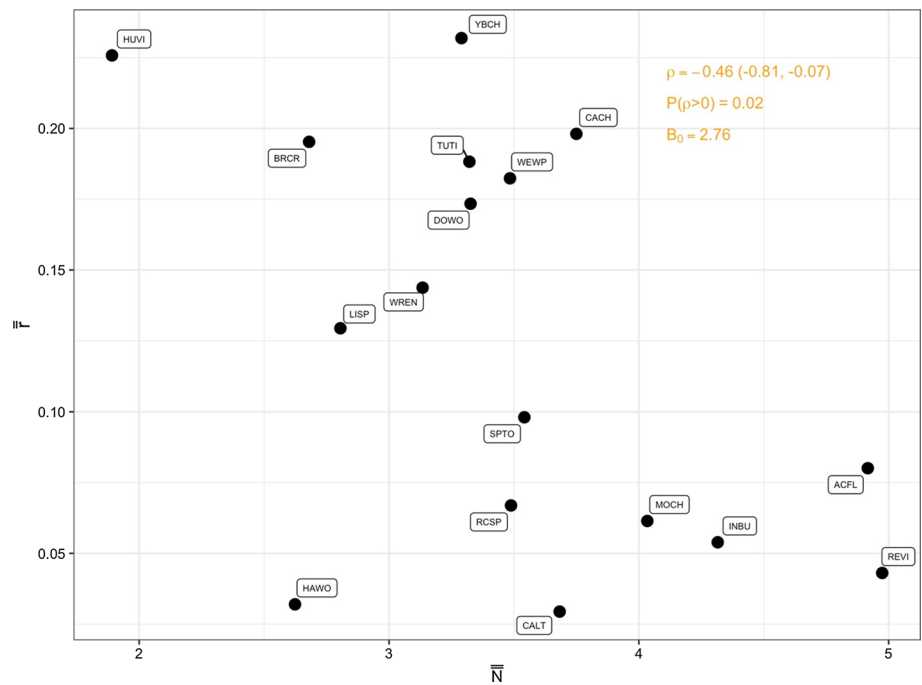


Fig. 5 Correlation between species level median abundance (\bar{N}), median intrinsic growth rate (\bar{r}). Every point represents a single species with the corresponding 4-letter code. ρ is the Pearson's correlation coefficient and its 95% credible interval is in parenthesis. $P(\rho > 0)$ indicates the probability that there is positive correlation between two parameters. B_0 is the Bayes factor against the null hypothesis that $\rho = 0$



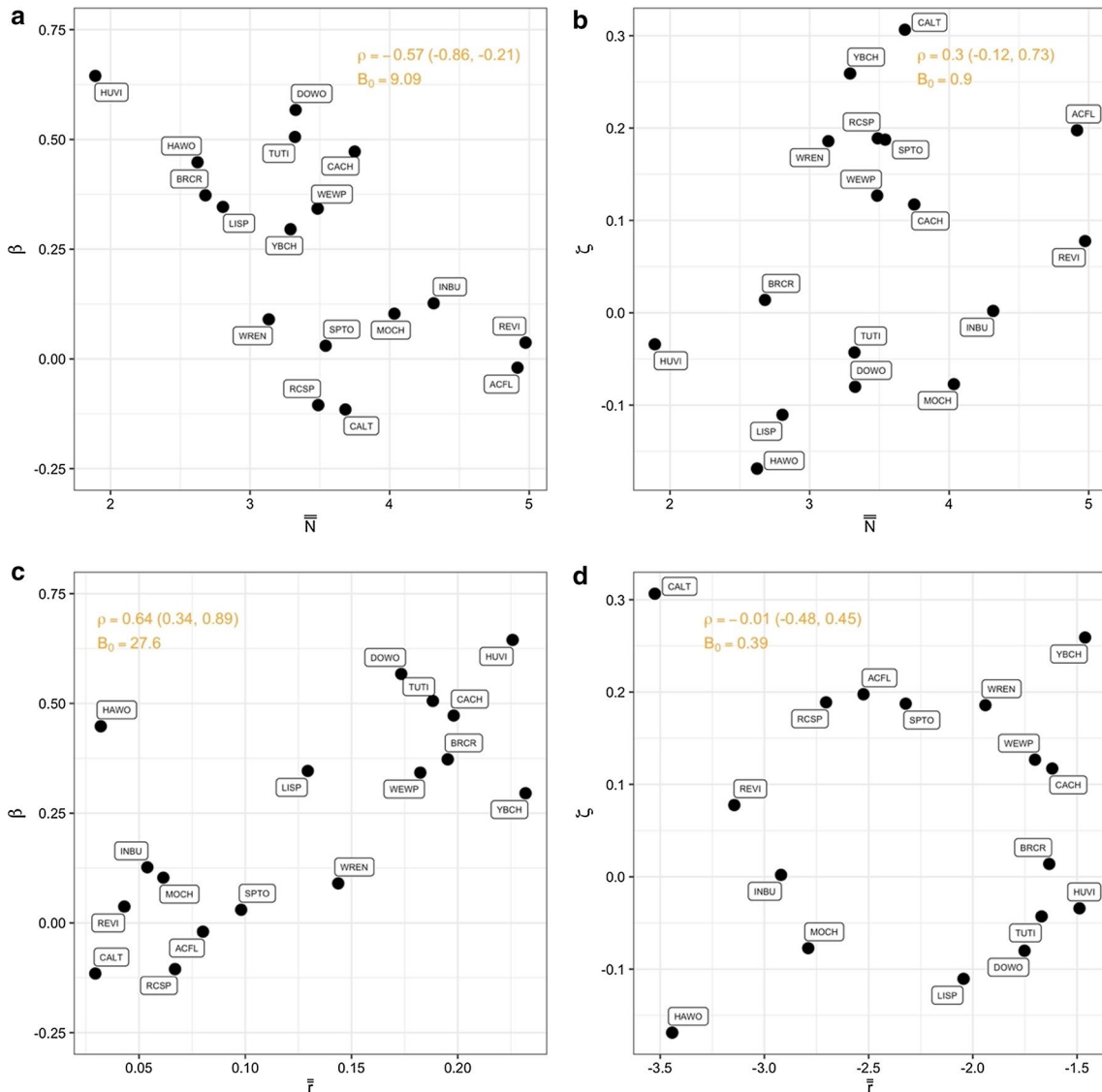


Fig. 6 Correlations between density dependence strength in survival (β), density dependence strength in fecundity (ζ), species level median abundance (\bar{N}), and median intrinsic growth rate (\bar{r}). Every point represents a single species with the corresponding 4-letter code.

ρ is the Pearson's correlation coefficient and its 95% credible interval is in parenthesis. $P(\rho > 0)$ indicates the probability that there is positive correlation between two parameters. B_0 is the Bayes factor against the null hypothesis that $\rho = 0$

populations in their breeding range may not correlate with the process of intra-specific competition in their wintering range. In these cases, a positive density dependence might represent a poor model fit. Analysis of more species in the MAPS dataset with years beyond 2008 might provide more definitive and generalizable answers to density dependent regulation of bird species. Here, we refrained from making generalizations regarding the prevalence of density dependence on bird species.

There are many different forms of density dependence; for example, Ricker, logistic, theta-logistic, contest, scramble, and ceiling (Akçakaya et al. 1999; Clark et al. 2010).

Each comes with their own set of assumptions and parameters. The fecundity model we use is a Poisson regression and exhibits similar properties to a Ricker model, where density dependence gets stronger in lower densities. However, the survival model is a logistic regression which produces opposite patterns to a Ricker model, where density dependence gets stronger in larger densities. Our model choice here was statistical; historically, survival is modeled with logistic regression on logit scale in mark-recapture models and count data with Poisson regression on log scale. The ecological assumptions that follow this statistical choice does not have to hold true for all species. Different forms

of density dependence than the framework we used might be more appropriate for species which we failed to detect density dependence. Using different links than logit and log can produce different ecological assumptions that is more appropriate for some species. It is also possible that different model structures might lead to better convergence for species with models that did not converge (Table S2). We believe an important future direction when analyzing the MAPS dataset for macroecological questions is to explore different forms of density dependence across species in order to detect not just the variability in density dependence strength but also variability in the form of density dependence as well.

There are several processes that can lead to a weak association between intrinsic growth rate and occupancy (Fig. 3). For example, if source-sink dynamics is the dominant process determining occupancy, then it is expected that many populations with negative intrinsic growth will be occupied and occupancy will not be strongly related to population growth. We do not have evidence to believe this is the main process in effect for the 17 bird species with negative density dependence, however, because majority of their populations have positive intrinsic growth (Appendix S1: Fig. S1b). Another process that can weaken the relationship between occupancy and intrinsic growth is local adaptation in range-restricted species as observed in mountainous bird species in the afro-tropical region (Symonds and Johnson 2006; Reif et al. 2006; Ferenc et al. 2016; Freeman 2019). These mountainous species are highly adapted to high elevation areas and can reach abundance levels and population growth similar to lower elevation species while still occurring across a narrower range. Although this mechanism can explain the lack of a positive abundance-occupancy relationship of specialist species with narrow ranges, it is not applicable to our study because the majority of the 17 bird species we modeled are wide-ranging across the US.

While vital rates mechanism is a framework that explains inter-specific patterns of abundance and occupancy, it also relies on the intra-specific assumption that abundance will follow the ecological niche of the species and that population abundances will be larger when closer to niche centroids (Martinez-Meyer et al. 2012). Ecological niches are directly related to intrinsic growth (Hutchinson 1978) and the relationship between abundance and niche centroid should reveal itself in the positive correlation between abundance and intrinsic growth among the population of a species. Here, we find no such evidence with the exception of Downy woodpecker (Fig. 4). There are several mechanisms proposed to explain such disassociation of abundance and intrinsic growth, for example, strong source-sink dynamics, Allee effects, and spatially variable density dependence (Osorio-Olvera et al. 2019; Holt 2020). We explained why source-sink dynamics is not a determining factor for the

abundance–occupancy relationship of these 17 bird species above, but we believe that both Allee effects and spatially variable density dependence can be responsible for weakening the relationship between population level growth and abundance and hence might be a contributing factor to the species level abundance–occupancy patterns we report. Unfortunately, both mechanisms require additional parameters to be fit and the statistical framework we used may not be feasible for their estimation.

The spatial response of intrinsic growth rate to environmental factors can be different among species. Holt et al. (1997) hypothesized that this difference will weaken the abundance–occupancy relationship because intrinsic growth rate will lose its positive association with occupancy. They present a simple case, where one species has a relatively steep response curve and its maximum growth can be high but it is also limited to a narrow range of an environmental gradient, whereas another species has a flatter response curve that reaches a lower maximum but it can exist on a wider range of the same environmental gradient. In this example, species with the higher intrinsic growth will not have higher occupancy. In our analysis, spatial response of intrinsic growth is quantified in the slopes estimated for the environmental variables in our framework (Eqs. 1a and 2a). There are two complications for comparing these slopes: (1) Because we use the principal component dimensions of environmental variables as covariates, the fitted slopes do not represent the response to same environmental variables; each dimension of each species can be different from others; and (2) the response to an environmental gradient that is described by Holt et al. (1997) is more akin to the concept of fundamental niche (Peterson 2011) but the framework we used here, or any other statistical method, may not be able to estimate the “true” response to environmental variability for the simple fact that species may not occur in every suitable site because of competitive exclusion. Inter-species biotic interactions are effectively missing from the vital rates mechanism. Differences in spatial variability of intrinsic growth rates among species, and whether these differences are mainly caused by density-independent factors or biotic interactions is an important future direction for abundance–occupancy relationships research.

Even though we found no relationship between abundance and occupancy among 17 bird species (Fig. 2b), we are not making any generalizations about the prevalence of positive abundance–occupancy relationships across different taxa. Detecting a positive abundance–occupancy relationship depends on the selected group of species; for example, Hurlbert & White (2007) found a pre-dominantly positive abundance–occupancy relationship across 298 bird species in US, but Novosolov et al. (2017) found no apparent pattern in 893 species across different biogeographical realms.

However, uncovering mechanisms and processes associated with abundance–occupancy patterns is just as important as determining the prevalence of these patterns across multiple taxa. We believe that small sub-groups of species, such as the 17 bird species in this study, can be used to explore the processes that affect the emergence of macroecological patterns. One limitation of this approach would be the length of time series. For example, most species in the MAPS program do not have enough recaptures to estimate data-sensitive demographic parameters such as intrinsic growth rate and density dependence. Also, long time series are necessary to detect the negative density dependence on population growth from population trends (Brook and Bradshaw 2006). As more data become available, these demographic parameters can be estimated for more species, and these species can be divided into further sub-groups that represent different distributions of demographic parameters among them. These sub-groups would provide a more complete picture for testing the predictions of vital rates mechanism. For example, a group that has similar density dependence strength should show a stronger positive abundance–occupancy relationship compared to another group with more variable density dependence strengths. Violation of this expected pattern would indicate other factors than vital rates determining abundance–occupancy relationships.

Patterns of distribution of life on Earth are interesting in themselves, but even more so when they are associated with, and explained by, mechanisms at different levels of biological organization. Holt et al. (1997) presented one such mechanism for the widely reported positive abundance–occupancy relationships. It is, however, likely that the abundance–occupancy patterns are simultaneously determined by dispersal, inter-specific and intra-specific interactions, species demography and response to environmental gradients, as well as the sampling schemes used to explore these relationships. Here, we only demonstrated the effect of within-population processes. Ideally, macroecological patterns would be explored in frameworks that include dynamics at all relevant scales, including processes that are at the population, metapopulation, and assemblage or community levels, and different sampling schemes. Such cross-scale frameworks would help us get a clearer picture of the conditions under which abundance–occupancy and other macroecological relationships emerge.

Supplementary Information The online version contains supplementary material available at <https://doi.org/10.1007/s00442-021-05085-5>.

Acknowledgements We thank Kevin Shoemaker for his valuable input. We thank the many volunteers who have contributed to the MAPS program and the Institute for Bird Populations for development and active curation of the MAPS dataset.

Author contribution statement BŞ originally formulated the idea and analyzed the data, BŞ and HRA developed the methodology and wrote the manuscript.

Funding This study was initiated under funding from the NASA Biodiversity Program (NNH10ZDA001N-BIOCLIM).

Availability of data and material The results of mark-recapture analysis are available at the Zenodo repository (<https://zenodo.org/record/4033457>). Information on how to obtain Mark-recapture data is available at <https://www.birdpop.org/pages/maps.php>.

Code availability R code for data manipulation and JAGS code for the mark-recapture framework are available at <https://github.com/bilgecansen/VitalRatesTest>.

Declarations

Conflicts of interest No conflict of interest to declare.

Ethics approval Not applicable.

Consent to participate Not applicable.

Consent for publication Not applicable.

References

- Akçakaya HR, Burgman MA, Ginzburg LR (1999) Applied population ecology: principles and computer exercises using RAMAS EcoLab 2.0. Sinauer Associates Sunderland, MA
- Albert SK, DeSante DF, Kaschube DR, Saracco JF (2016) MAPS (monitoring avian productivity and survivorship) data provide inferences on demographic drivers of population trends for 158 species of North American Landbirds. *North American Bird Bander* 41:12–19
- Behnke R, Vavrus S, Allstadt A et al (2016) Evaluation of down-scaled, gridded climate data for the conterminous United States. *Ecol Appl* 26:1338–1351. <https://doi.org/10.1002/15-1061>
- Blackburn TM, Cassey P, Gaston KJ (2006) Variations on a theme: sources of heterogeneity in the form of the interspecific relationship between abundance and distribution. *J Anim Ecol* 75:1426–1439. <https://doi.org/10.1111/j.1365-2656.2006.01167.x>
- Blackburn TM, Gaston KJ, Quinn RM et al (1997) Of mice and wrens: the relation between abundance and geographic range size in British mammals and birds. *Philos Trans R Soc Lond B Biol Sci* 352:419–427. <https://doi.org/10.1098/rstb.1997.0030>
- Bock CE, Ricklefs RE (1983) Range size and local abundance of some North American Songbirds: a positive correlation. *Am Nat* 122:295–299. <https://doi.org/10.1086/284136>
- Borregaard MK, Rahbek C (2010) Causality of the relationship between geographic distribution and species abundance. *Q Rev Biol* 85:3–25. <https://doi.org/10.1086/650265>
- Brook BW, Bradshaw CJ (2006) Strength of evidence for density dependence in abundance time series of 1198 species. *Ecology* 87:1445–1451
- Brown JH (1984) On the relationship between abundance and distribution of species. *Am Nat* 124:255–279. <https://doi.org/10.1086/284267>

- Brown JH (1995) *Macroecology*. University of Chicago Press, Chicago
- Clark F, Brook BW, Delean S et al (2010) The theta-logistic is unreliable for modelling most census data. *Methods Ecol Evol* 1:252–263. <https://doi.org/10.1111/j.2041-210X.2010.00029.x>
- Conrad KF, Perry JN, Woiwod IP (2001) An abundance-occupancy time-lag during the decline of an arctiid tiger moth. *Ecol Lett* 4:300–303. <https://doi.org/10.1046/j.1461-0248.2001.00234.x>
- Dail D, Madsen L (2011) Models for estimating abundance from repeated counts of an open metapopulation. *Biometrics* 67:577–587. <https://doi.org/10.1111/j.1541-0420.2010.01465.x>
- Ferenc M, Fjeldså J, Sedláček O et al (2016) Abundance-area relationships in bird assemblages along an Afrotropical elevational gradient: space limitation in montane forest selects for higher population densities. *Oecologia* 181:225–233. <https://doi.org/10.1007/s00442-016-3554-0>
- Freckleton RP, Noble D, Webb TJ (2006) Distributions of habitat suitability and the abundance-occupancy relationship. *Am Nat* 167:260–275. <https://doi.org/10.1086/498655>
- Freeman BG (2019) No evidence for a positive correlation between abundance and range size in birds along a New Guinean elevational gradient. *Emu Austral Ornithol* 119:308–316. <https://doi.org/10.1080/01584197.2018.1530062>
- Gaston KJ, Blackburn TM (2000) *Pattern and process in macroecology*. Blackwell Science, Oxford, OX ; Malden, MA, USA
- Gaston KJ, Blackburn TM, Lawton JH (1997) Interspecific abundance-range size relationships: an appraisal of mechanisms. *J Anim Ecol* 66:579. <https://doi.org/10.2307/5951>
- Guo Q, Brown JH (2000) Abundance and distribution of desert annuals: are spatial and temporal patterns related? *J Ecol* 88:551–560. <https://doi.org/10.1046/j.1365-2745.2000.00466.x>
- Hanski I (1982) Dynamics of regional distribution: the core and satellite species hypothesis. *Oikos* 38:210. <https://doi.org/10.2307/3544021>
- Holt RD (2020) Reflections on niches and numbers. *Ecography* 43:387–390. <https://doi.org/10.1111/ecog.04828>
- Holt RD, Lawton JH, Gaston KJ, Blackburn TM (1997) On the relationship between range size and local abundance: back to basics. *Oikos* 78:183. <https://doi.org/10.2307/3545815>
- Hurlbert AH, White EP (2007) Ecological correlates of geographical range occupancy in North American birds. *Glob Ecol Biogeogr* 16:764–773. <https://doi.org/10.1111/j.1466-8238.2007.00335.x>
- IUCN (2021) The IUCN red list of threatened species. Version 2021–2. <https://www.iucnredlist.org>. Downloaded on 01/08/2021
- Hutchinson GE (1978) *An introduction to population ecology*. Yale University Press, New Haven
- Jeffreys H (1983) *Theory of probability*, 3rd ed. Clarendon Press ; Oxford University Press, Oxford [Oxfordshire]; New York
- Kass RE, Raftery AE (1995) Bayes factors. *J Am Stat Assoc* 90:773–795. <https://doi.org/10.1080/01621459.1995.10476572>
- Kuno E (1991) Some strange properties of the logistic equation defined with r and K : Inherent defects or artifacts? *Res Popul Ecol* 33:33–39. <https://doi.org/10.1007/BF02514572>
- Lacy RC, Bock CE (1986) The correlation between range size and local abundance of some North American Birds. *Ecology* 67:258–260. <https://doi.org/10.2307/1938527>
- Lynch HJ, Fagan WF (2009) Survivorship curves and their impact on the estimation of maximum population growth rates. *Ecology* 90:1116–1124
- Martinez-Meyer E, Diaz-Porrás D, Peterson AT, Yanez-Arenas C (2012) Ecological niche structure and rangewide abundance patterns of species. *Biol Lett* 9:20120637–20120637. <https://doi.org/10.1098/rsbl.2012.0637>
- Maurer EP, Wood AW, Adam JC et al (2002) A long-term hydrologically based dataset of land surface fluxes and states for the conterminous United States. *J Clim* 15:3237–3251
- Novosolov M, Rodda GH, North AC et al (2017) Population density-range size relationship revisited. *Glob Ecol Biogeogr* 26:1088–1097. <https://doi.org/10.1111/geb.12617>
- Osorio-Olvera L, Soberón J, Falconi M (2019) On population abundance and niche structure. *Ecography* 42:1415–1425. <https://doi.org/10.1111/ecog.04442>
- Peterson AT (ed) (2011) *Ecological niches and geographic distributions*. Princeton University Press, Princeton
- Reif J, Hořák D, Sedláček O et al (2006) Unusual abundance-range size relationship in an Afrotropical bird community: the effect of geographical isolation? *J Biogeogr* 33:1959–1968. <https://doi.org/10.1111/j.1365-2699.2006.01547.x>
- Russell MP, Lindberg DR (1988) Real and random patterns associated with molluscan spatial and temporal distributions. *Paleobiology* 14:322–330. <https://doi.org/10.1017/S0094837300012070>
- Ryu HY, Shoemaker KT, Kneip É et al (2016) Developing population models with data from marked individuals. *Biol Cons* 197:190–199. <https://doi.org/10.1016/j.biocon.2016.02.031>
- Symonds MRE, Johnson CN (2006) Range size-abundance relationships in Australian passerines. *Glob Ecol Biogeogr* 15:143–152. <https://doi.org/10.1111/j.1466-822X.2005.00198.x>
- Wilson PD (2008) The pervasive influence of sampling and methodological artefacts on a macroecological pattern: the abundance-occupancy relationship. *Glob Ecol Biogeogr* 17:457–464. <https://doi.org/10.1111/j.1466-8238.2008.00385.x>